Biomaterials 33 (2012) 5696–5705

Contents lists available at SciVerse ScienceDirect

Biomaterials

journal homepage: www.elsevier.com/locate/biomaterials

The influence of genetic factors on the osteoinductive potential of calcium phosphate ceramics in mice

Ana M.C. Barradas [a], Huipin Yuan [a,b], Johan van der Stok [c], Bach Le Quang [d], Hugo Fernandes [a], Anindita Chaterjea [a], Marieke C.H. Hogenes [e], Kathy Shultz [d], Leah Rae Donahue [d], Clemens van Blitterswijk [a], Jan de Boer [a,*]

[a] Department of Tissue Regeneration, MIRA Institute for Biomedical Technology and Technical Medicine, University of Twente, Drienerlolaan 5, 7522 NB Enschede, The Netherlands
[b] Progentix Orthobiology BV, Bilthoven, The Netherlands
[c] Orthopedic Research Laboratory, Department of Orthopaedics, Erasmus MC, University Medical Center Rotterdam, Rotterdam, The Netherlands
[d] The Jackson Laboratory, Bar Harbor, ME 04609, USA
[e] Laboratory for Pathology, East Netherlands, Burgemeester Edo Bergsmalaan 1, 7512 AD Enschede

ARTICLE INFO

Article history:
Received 15 March 2012
Accepted 7 April 2012
Available online 15 May 2012

Keywords:
Calcium phosphate
BMP (bone morphogenetic protein)
Osteoblast
Bone

ABSTRACT

The efficacy of calcium phosphate (CaP) ceramics in healing large bone defects is, in general, not as high as that of autologous bone grafting. Recently, we reported that CaP ceramics with osteoinductive properties were as efficient in healing an ilium defect of a sheep as autologous bone graft was, which makes this subclass of CaP ceramics a powerful alternative for bone regeneration. Although osteoinduction by CaP ceramics has been shown in several large animal models it is sporadically reported in mice. Because the lack of a robust mouse model has delayed understanding of the mechanism, we screened mice from 11 different inbred mouse strains for their responsiveness to subcutaneous implantation of osteoinductive tricalcium phosphate (TCP). In only two strains (FVB and 129S2) the ceramic induced bone formation, and in particularly, in FVB mice, bone was found in all the tested mice. We also demonstrated that other CaP ceramics induced bone formation at the same magnitude as that observed in other animal models. Furthermore, VEGF did not significantly increase TCP induced bone formation. The mouse model here described can accelerate research of osteoinductive mechanisms triggered by CaP ceramics and potentially the development of therapies for bone regeneration.

1. Introduction

Porous calcium phosphate ceramics are frequently used in orthopaedic surgery as graft material to heal bone defects. Their chemical composition is similar to the natural mineral of the bone. In general, CaP ceramics are considered osteoconductive, meaning that they are able to facilitate bone infiltration from the bone surrounding the defect. A subclass of CaP ceramics also has been recognized as being osteoinductive [1–5]. We define osteoinductivity of a biomaterial by the potential of the material to induce bone formation while implanted in an animal at ectopic sites (e.g. subcutaneously or intramuscularly). The specific biological response triggered by osteoinductive materials that results in bone formation is, however, poorly known. Nonetheless, their osteoinductive capacity has been often linked with specific physico-chemical properties such as chemical composition, scaffold architecture and micro- and nano- structure.

We recently reported that ceramics with different physico-chemical properties induce bone formation in dogs with different degrees of efficacy: tricalcium phosphate (TCP) induced more bone formation than hydroxyapatite (HA). In the same study, we also demonstrated that TCP grafting of an ilium defect in sheep is as effective as the most frequently used therapies for human patients: autologous bone grafting and recombinant human BMP-2 (rhBMP-2). This finding strongly revealed the potential of osteoinductive ceramics to heal bone defects in clinical scenarios, overcoming the disadvantages of donor tissue morbidity and pain associated with autologous bone graft and issues related to cost and safety associated with the use of rhBMP-2 [6]. However, in order to bring these materials to the clinic, full understanding of the mechanism of action would help to determine their efficacy, efficiency and safety.

The immune system has been associated with the physiological response leading to CaP ceramic induced bone formation. It is hypothesized, for instance, that materials with different surface

* Corresponding author. Tel.: +31 53 489 3400; fax: +31 53 489 2150.
E-mail address: j.deboer@utwente.nl (J. de Boer).

0142-9612/$ – see front matter © 2012 Elsevier Ltd. All rights reserved.
doi:10.1016/j.biomaterials.2012.04.021

characteristics, e.g. surface roughness or micro-topography, will induce different responses in macrophages. For instance, prostaglandin E2 (PGE2) was secreted by macrophages only when in contact with a micro rough- and not when in contact with a smooth surface. Furthermore, PGE2 enhanced chemotaxis and osteogenic differentiation of human bone barrow derived mesenchymal stromal cells [7]. *In vivo*, PGE2 enhances bone formation through the PGE receptor EP4 [8] and it can also induce osteoclast formation and bone resorption [9]. Harada and colleagues [10] also showed that among all different CaP granules tested, only HA dried at 110 °C (HA_{110}) induced expression of PGE2 by primary human macrophages/monocytes cells, whereas HA sintered at 900 and 1200 °C did not. The authors from the study also noticed that although all granules were similar in size, HA_{110} presented a more irregular shape and sharper edges than the other CaP granules [10]. Similar studies have been conducted *in vitro* [11,12] but the question of whether macrophages functionally contribute to *in vivo* bone formation by osteoinductive CaP biomaterials is not yet answered. Some authors have hypothesized though that the origin of the cells that deposit de novo bone is of vascular nature [13–15], based on the observation that cells of vascular origin appear in the vicinity of the ceramic implant. Therefore the role of blood vessels in osteoinduction could be more than the already essential transport of nutrients and gases to the tissue in the pores [16].

Although some progress has been made in the past 20 years, the mechanism of action of osteoinductive CaPs is not clear, partially due to limitations associated with the existent *in vitro* and *in vivo* models. Pre-clinical models with large animals, such as sheep, dogs and goats are more often used than small animal models, since osteoinduction by CaP ceramics in mice or rats is considered a sporadic event [17]. Nevertheless, a robust mouse model would be preferred over large animal models, since these are more expensive than smaller ones and require experienced surgeons. Mouse models could also accelerate research due to easy access to a wide variety of inbred strains, broader choice of complementary research tools, such as available drugs for functional assays, and antibodies for tissue characterization. Furthermore, there are many genetic tools available for mouse research, enabling gene identification via quantitative trait locus (QTL) coupled with genetic engineering to manipulate the mouse genome to prove causation of gene effects. Application of these methodologies in mice could potentially lead to identification of genetic loci associated with bone formation never before identified.

We previously obtained proof of principle that CaP-triggered osteoinduction is possible in mice [18]. Bone formation was observed in Swiss white mice implanted with biphasic calcium phosphate (BCP). The amount of bone formed was limited, with less than 1% of bone area per scaffold area and was only observed in 3/16 animals tested. Moreover, Swiss white is an outbred mouse strain, whereas inbred mice are preferred as mentioned before. More recently, Yang and colleagues [19] tested BCP ceramics in the muscle of the posterior legs of inbred Balb/C mice and found bone in all explants. Although a promising result, the distance between the leg muscle and native bone tissue in a mouse is short and it can be argued whether osteoconduction from bone tissue into the implant played a role or not.

These findings suggest that the induction of bone formation in mice induced by a CaP ceramic might be strain dependent. Indeed, Malusic and colleagues [20] reported that ectopic bone formation was dependent on genetic background, although in their case the implants were pieces of bone matrix. As BMPs are thought to be responsible for the osteoinductive potential of demineralized bone matrix, this further suggests that in addition to differences in osteoinduction by CaP in different strains there are also differences in BMP induction.

In the search for a suitable mouse model for the study of CaP osteoinductive ceramics, we investigated the response of 11 different mouse strains to subcutaneous implantation of CaP ceramics, based on the assumption that genetic background will influence the propensity of the materials to induce bone tissue.

2. Materials and methods

2.1. Materials fabrication and sterilization

HA ceramics were prepared from HA powder (Merck) using the dual-phase mixing method and sintered at 1250 °C for 8 h according to a previously described method [21]. BCP ceramics were fabricated using the H_2O_2 method using in-house made calcium-deficient apatite powder and sintered at 1150 °C (BCP1150) and 1300 °C (BCP1300), respectively [22]. The method used to synthesize the BCP ceramics was also used for preparation of β-TCP (for simplicity abbreviated to TCP). TCP ceramics were prepared from TCP powder (Plasma Biotal) and sintered at 1050 °C. Ceramic blocks (4 × 4 × 4 mm) were cut, cleaned ultrasonically with acetone, 70% ethanol and demineralized water (dH_2O), dried at 80 °C and autoclaved for sterilization.

2.2. Growth factor incorporation into the ceramic blocks

Five μg of rh-BMP-2 dissolved in demineralized water (dH_2O) (Shanghai Rebone Biomaterials Co. Ltd) were pipetted per block of TCP (refered to as TCPb). TCPb was vacuum dried in a sterile environment for two days. In the case of rhVEGF (Invitrogen), 1.8 μg was loaded in 25 μl of dH_2O per block of TCP, just prior to implantation.

2.3. Ceramic implantation in mice

Ceramic blocks were implanted in 6–7 weeks old mice. Name and providers of mouse-inbred strains, as well as the respective abbreviations used throughout this manuscript, are given in Table 1. Preoperative analgesia (Temgesic, Schering-Plough BV) was injected subcutaneously (s.c.) followed by general anesthesia consisting of a mix of 1–3% isoflurane (IsoFlo, Abbott Lab.) in oxygen (Linde Gas). After shaving the back and disinfection of the skin with ethanol, small incisions were created on the dorsal sides. Subcutaneous pockets were opened in these incisions with blunt scissors. Ceramic blocks were inserted into the pockets, which were then closed with sutures. Animals were allowed to recover from anesthesia before returning to the cages. Mice were killed with either CO_2 inhalation or cervical dislocation. Skin was immediately opened to retrieve the ceramic blocks (explants). All animal experiments were performed following approval of the Animal Experiments Committee Utrecht, The Netherlands.

2.4. Femora extraction and micro-CT scanning

Three C3H, CBA, FVB and 129S2 mice, aged between 6 and 7 weeks, were selected for micro-CT scanning. The right femur of each mouse was extracted, cleaned from skin and soft tissue and fixed with 1.5% glutaraldehyde in 0.14 M cacodylate buffer, pH 7.3. Micro-CT scans were acquired using the SkyScan 1076 scanner (Kontich, Belgium) with a 9 μm-resolution protocol (60 kV energy, 170 μA current, 1.0 mm Al filter). CT shadow projection images were converted into a three dimensional (3D) reconstruction of cross-sectional images in bitmap files using volumetric reconstruction software NRecon version 1.6 (SkyScan, Belgium). With Dataviewer 1.4, a segment of the distal metaphysis (10 mm) was selected as region of interest. To distinguish calcified tissue from non-calcified tissue and noise, the reconstructed grayscale images were segmented by an automated algorithm using local thresholds, resulting in a 3D dataset consisting of stacked black/white cross-sections. Cortical and trabecular bone were subsequently automatically separated

Table 1
Inbred mouse strains and their respective providers.

Mice strain	Abbreviations	Provider
C3H/HeNHsd	C3H	Harlan Laboratories, Inc.
DBA/1OlaHsd	DBA1	
DBA/2OlaHsd	DBA2	
CBA/CaOlaHsd	CBA	
BALB/cOlaHsd	BALBc	
C57BL/6JOlaHsd	C57BL6	
FVB/NCrl	FVB	Charles River Laboratories
129S2/SvPasCrl	129S2	International, Inc.
SJL/JOrlCrl	SJL	
CB17/Icr-*Prkdc*^{scid}/IcrCrl	CB17	
A/J	A/J	The Jackson Laboratory

using in-house software. Trabecular architecture of the metaphysic was characterized by determining the trabecular bone volume fraction (BV/TV), which is the ratio of trabecular bone volume over endocortical tissue volume, connectivity density, structural model index, trabecular thickness and trabecular separation were also calculated.

2.5. Histochemical stainings

After fixation with 1.5% v/v glutaraldehyde in 0.14 M cacodylate buffer, pH 7.3, explants were dehydrated with several microwave runs at 70 °C for 1 h. For each run, implants were immersed in either 70% ethanol in dH_2O, 80% ethanol in dH_2O, JFC (Milestone Medical Technologies S.r.l.) or 100% ethanol in dH_2O (2 times). After dehydration, samples were placed in glass jars, immersed in methyl methacrylate (MMA) for 16 h at 4 °C, and the next day MMA was refreshed. After 2 days in a water bath at 37 °C, samples were removed from the glass jars and sectioned. Tissue sections of approximately 10–15 μm thickness were obtained with a Leica SP 1600 and stained with 1% methylene blue (Sigma–Aldrich) in 0.1 M borax (pH 8.5) and 0.3% basic fuchsin solutions (Sigma–Aldrich).

2.6. Bone quantification

Three nonconsecutive sections per sample per animal were digitally scanned and quantified using Adobe Photoshop CS5 Extended (version 12.0.4, Adobe Systems Inc.) as follows: bone and scaffold areas were differentially pseudo-colored and the ratio between pixels of each color converted to percentage of bone area per scaffold area (bA/sA). Fig. S1 summarizes the number of implanted, explanted and analysed blocks.

2.7. Statistical analysis

Statistical analysis performed for the individual experiments is specified in the figure legend. Error bars indicate standard deviation. For all figures the following applies: * = $p < 0.05$; ** = $p < 0.01$; *** = $p < 0.001$; *ns* = non significant.

3. Supplementary materials and methods

3.1. C2C12 expansion and culture on ceramic blocks

Cells from the mouse myoblast cell line C2C12 were expanded on tissue culture polystyrene plates at an initial seeding density of 1000 cells cm^{-2} in Basic Medium (BM), consisting of Dulbecco's Modified Eagle Medium (DMEM, Gibco), 10% foetal bovine serum (Lonza), 100 U/ml penicillin and 100 mg/ml streptomycin (Gibco). Cells were harvested at approximately 80% confluency and resuspended in fresh BM. Six hundred thousand cells in 100 μl BM were pipetted on TCP or TCPb and allowed to attach for 3 h. Culture medium was refreshed every 2–3 days. All experiments were performed in a 5% CO_2 humid atmosphere at 37 °C.

3.2. DNA concentration and alkaline phosphatase activity

Total DNA was assessed with CyQuant Cell Proliferation Assay kit (Invitrogen). Culture medium was aspirated from the samples and after rinsing with PBS transferred to tubes containing 500 μl lysis buffer (prepared according to manufacturer's instructions). After 1 freeze/thaw cycle at −80 °C, samples were ultra-sonicated to ensure recovery of all cellular material present in the pores. After centrifugation, the supernatant was mixed with 1) CyQuant GR dye (1×) 1:1 in a 96 well microplate and incubated for 5 min or 2) CDP-Star, ready-to-use (Roche Applied Science) substrate 1:3 in a 96 well microplate and incubated for 30 min. Fluorescence measurements for DNA quantification were done at an excitation and emission wavelength of 480 and 520 nm, respectively, using a spectrophotometer (Perkin Elmer Corporation). For the CDP-Star assay, chemiluminescence measurement was set at 466 nm.

3.3. Ceramics decalcification and paraffin embedding

After fixation in 10% formalin neutral buffered solution (Sigma–Aldrich Co.), explants were rinsed in PBS, embedded in 3% (v/v) agarose in PBS and left to solidify at room temperature (RT). The embedded samples were decalcified in 12.5% (v/v) ethylenediamine tetraacetic acid (EDTA) in water. Total decalcification was confirmed with X-rays (Faxitron, Vet Path Services, Inc.). Afterwards, samples were incubated in different solutions under the following conditions: 4% formalin (90 min, 37 °C), 50% ethanol (30 min, 37 °C), 70% ethanol (30 min, 37 °C), 100% ethanol (5 × 30 min, 37 °C), xylene (2 × 45 min, 37 °C) and paraffin (4 × 1 h, 62 °C). Paraffin (Adamas) embedded samples were cut using a microtome (Microm HM 335 E, Thermo-Fisher Scientific).

3.4. Immunohistochemistry

Slides from the outer side and at approximately middle height of the blocks were all counter stained with hematoxylin and eosin (Richard-Allen) as well as CD3 (AO452, Dako, diluted 1:100) or CD20 antibodies (Santa Cruz, diluted 1:50). For CD20 antibody staining, antigen retrieval was performed with EDTA buffer, pH 9.0 for 20 min at 100 °C. Samples were incubated with the primary antibody for 1 h at RT and incubated with the secondary antibody rabbit anti-goat (horseradish peroxidase conjugated, 1:100) for 30 min at RT. Slides were developed with DAB for 10 min at RT. In the case of CD3, antigen retrieval was performed at 99 °C for 20 min, samples were incubated with the primary antibody for 15 min at RT and with the secondary antibody rabbit anti-goat (horseradish peroxidase conjugated, 1:100) for 30 min at RT. Slides were developed with the bond polymer refine detection kit (Leica, DS9800).

4. Results

4.1. Bone induction by rhBMP-2 adsorbed onto TCP

To evaluate whether the mouse genetic background determines the efficacy of ectopic bone formation, we implanted rhBMP-2 adsorbed onto TCP subcutaneously in 11 different inbred mouse strains (Table 1), since this cytokine has ectopic osteoinductive ability in different rodent models [23–27]. Prior to *in vivo* evaluation, however, the activity of rhBMP-2 adsorbed onto TCP was tested with C2C12 cells *in vitro*. C2C12 cells are known to express alkaline phosphatase (ALP) in response to rhBMP-2 [28]. Therefore cells were cultured on TCP or TCPb in BM for three days, after which ALP activity and cell numbers were measured. In TCPb, C2C12 cells exhibited 18 times higher ALP activity per cell than when cultured in TCP alone, confirming that rhBMP-2 was still active while adsorbed onto the porous ceramics (Fig. S2).

Next, TCPb was implanted subcutaneously in all mouse strains (Table 1). Twelve weeks after implantation, animals were sacrificed, samples explanted, slides were cut and stained with basic fuchsin (mineralized tissue) and methylene blue (counterstaining).

TCPb induced bone formation in every mouse of all strains. As can be seen in Fig. 1, representative for all strains, typical morphology of mature lamellar bone was observed in contact with the TCPb surface (for reference see Fig. S3). Mineralized bone matrix (stained pink) was observed, embedding osteoblasts resting in lacunae (osteocytes). The pores of the ceramic blocks were filled with bone marrow, characterized by the presence of nucleated heamatopoetic cells and large amounts of mature adipocytes.

Interestingly, we observed differences in the amount of bone among the different mouse strains (Fig. 2), confirming that bone induction by rhBMP-2 is dependent on genetic background. Bone per scaffold area ranged from 7 ± 3.2% (FVB) to 27 ± 11% (C3H). Interestingly, strains with a close genetic background, such as DBA1 and DBA2 exhibited a large statistically significant difference (9 and 20% respectively).

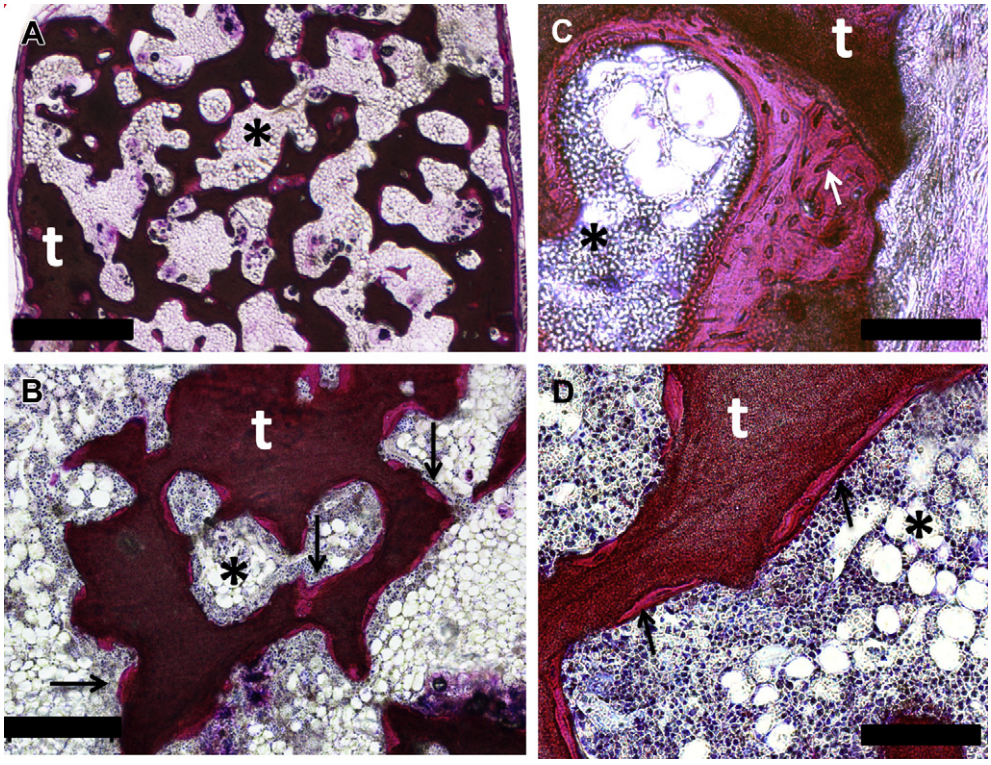

Fig. 1. Representative images of bone formation induced by TCPb. A and B) Bright pink mineralized bone tissue (black arrows) was observed in contact with TCP (t) aligning the pores filled with bone marrow (*). C) Osteocytes (white arrows) were present in the mineralized bone matrix. D) Detail of bone marrow (*) and osteoblasts (black arrows). Scale bars represent 1 mm (A), 200 μm (B) and 100 μm (C and D).

This result shows that all tested mouse strains can form bone in subcutaneous pockets and that furthermore, the efficacy of bone formation induced by TCPb depends on the genetic background.

4.2. Bone induction by TCP

In contrast with the results found for TCPb, but further confirming genetic background dependence, bone formation induced by TCP occurred in only two out of 11 mouse strains: FVB and 129S2.

In both strains, bone tissue was mostly observed at the periphery of the ceramic block, and in contact with the scaffold (Fig. 3A). Similarly to results obtained with TCPb, mature lamellar bone had developed, with characteristic osteoblasts rimming the lamellar bone (Fig. 3B) and osteocytes within the lamellar bone (Fig. 3D). In a few cases, cavities filled with bone marrow were observed, in both mouse strains (Fig. 3C). Furthermore, we did not observe cartilage tissue in any of the explanted sections.

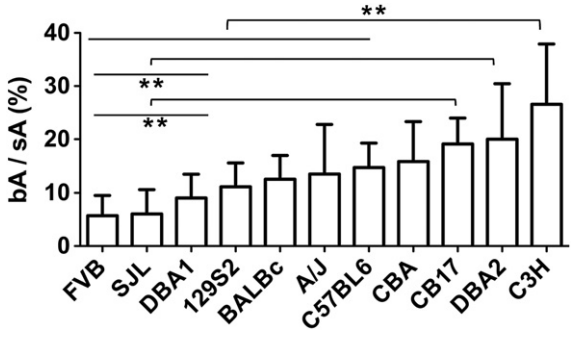

Fig. 2. Bone formation induced by TCPb. TCP loaded with rhBMP-2 was implanted subcutaneously in mice from 11 different mouse strains. Twelve weeks later, samples were explanted, bone tissue quantified from tissue sections and presented as % bA/sA. FVB (7%) showed the lowest average amount of bone tissue whereas C3H the highest (27%). Statistical analysis was performed with One-Way analysis of Variance (ANOVA) and Tukey's multiple comparison test ($p < 0.05$).

Although mature lamellar bone tissue was found in both strains, the incidence was different. In FVB mice, TCP induced bone in all mice (6/6) whereas in 129S2 the incidence was lower: 4/5 (Fig. S1). TCP explants from FVB also showed an average bA/sA higher than that of 129S2: 2.8 ± 4.6% and 0.2 ± 0.26% respectively (Fig. 4).

Thus, we successfully identified two mouse strains, FVB and 129S2, in which TCP induced bone formation subcutaneously, showing that the genetic background of individuals is a key element in the osteogenic response to synthetic materials.

4.3. Bone architecture

In order to investigate whether TCPb or TCP bone inductive capacity in specific mouse strains could be correlated with bone features inherent to each strain, femora from FVB (lowest induction by TCPb and highest by TCP), 129S2 (lowest induction by TCP), CBA and C3H (highest induction by TCPb) were extracted and evaluated by micro-CT scanning.

Based on the distal metaphysis region from 3D reconstructed images of the femora, several parameters were evaluated: structural model index (prevalence of a particular trabecular shape), trabecular separation, trabecular thickness, connectivity density (number of redundant connections between trabecular structures per unit volume, which can be associated with trabecular strength [29]) and the percentage of bone in a defined volume of interest (% of bone volume, %BV), which can be seen as a true measurement of bone mineral density (BMD).

Statistically significant differences were not observed for any of the parameters measured between the mouse strains (Fig. 5). This

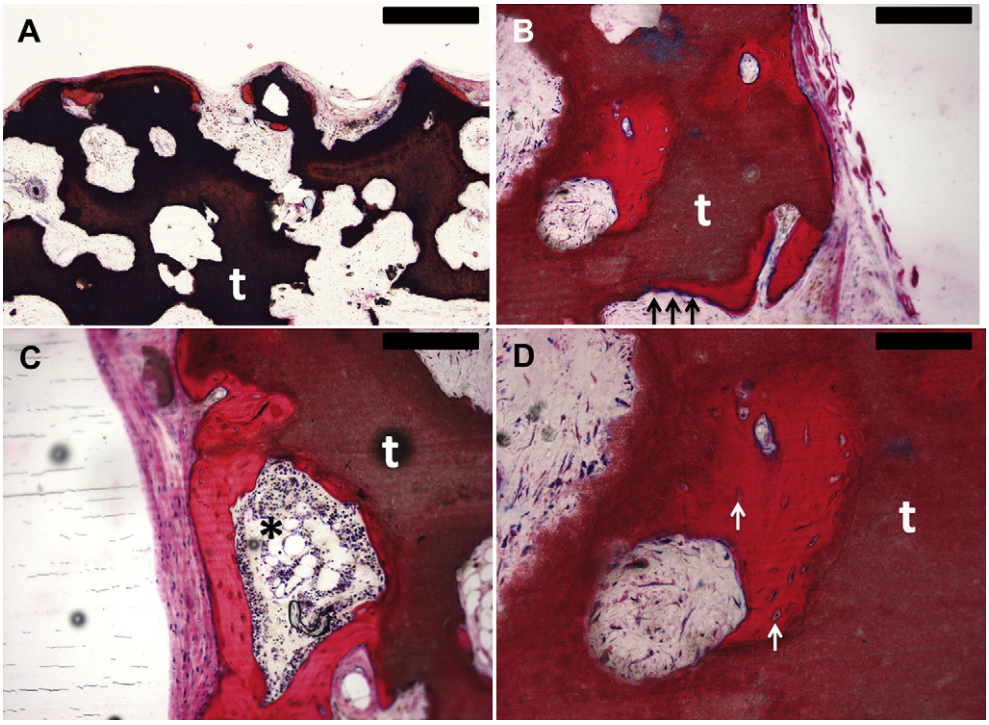

Fig. 3. Representative images of bone formation induced by TCP in FVB and 129S2. Mineralized bone tissue (red) was observed mostly at the periphery of the implant (A) and in contact with the scaffold (t), aligned by osteoblasts (black arrows) (B). C) Detail of cavity filled with bone marrow (*). D) Detail of osteocytes (white arrows). Scale bars represent 400 μm (A), 200 μm (B and C) and 100 μm (D).

suggests that the genetic and molecular mechanisms that regulate bone induction by TCPb or TCP are not correlated with strain specific differences in bone parameters of 6–7 week old mice from these inbred strains.

4.4. Ectopic bone formation in response to different ceramics

After identifying the more responsive genetic background to TCP osteoinductivity, FVB, we implanted different CaP ceramics in these mice to evaluate whether any block shaped CaP ceramic would induce ectopic bone formation or whether that response was exclusive of a particular setting of physico-chemical characteristics.

Therefore, this time, besides TCP, we also implanted HA, different in terms of chemistry and microstructural features, BCP1150 and BCP1300. The last two possess equal chemistry, though BCP1150 possesses more micropores and smaller grains than BCP1300. For a detailed characterization of these materials, the reader is referred to Yuan et al. [3].

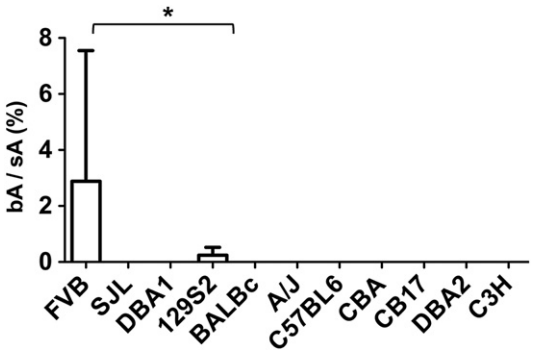

Fig. 4. Bone formation induced by TCP. TCP was implanted subcutaneously in mice from 11 different mouse strains. Twelve weeks later, samples were explanted, bone tissue quantified from tissue sections and presented in the image as % relative to scaffold area. Bone formation was observed in FVB (2.8 ± 4.6%) and 129S2 (0.2 ± 0.26%) mice. Statistical analysis was performed with One-Way ANOVA and Tukey's multiple comparison test ($p < 0.05$).

After 12 weeks of implantation, BCP1300 and HA did not induce bone formation in FVB mice. In contrast, BCP1150 and TCP induced bone formation. There were no statistically significant differences in the amount of bone tissue induced by TCP and BCP1150 (Fig. 6 B) though bone incidence, defined as the ratio between the number of explants with bone (N_b) and the number of total explants (N_t) (N_b/N_t), was different (3/4 and 5/5 for BCP1150 and TCP respectively, Fig. 6A).

Similarly to what was previously described for TCP, bone was mainly found at the periphery of the implant but was also seen in contact with the scaffold (Fig. 6C). Osteocytes and osteoblasts were also observed in BCP1150 explants but bone marrow cavities were not.

Furthermore, although all explants were perfused by blood vessels distributed throughout the implants, vascularization seemed to be more pronounced in the case of TCP and BCP1150, although no quantitative data is available to support these observations. Interestingly, in the case of BCP1150, blood vessels were often surrounded by adipocytes. In the pores of BCP1300 and HA explants, mainly fibrous tissue was observed (Fig. 7).

TCP and BCP1150 induced ectopic bone formation in FVB mice whereas BCP1300 and HA did not. This suggests that the biological response that leads to bone formation in FVB mice is dependent on the materials' specific characteristics and not a random phenomenon of heterotopic ossification.

4.5. Role of vascularization in osteoinduction

Bone formation was observed in both TCP and BCP1150 explants, mainly at the periphery of the ceramic. Immediately after

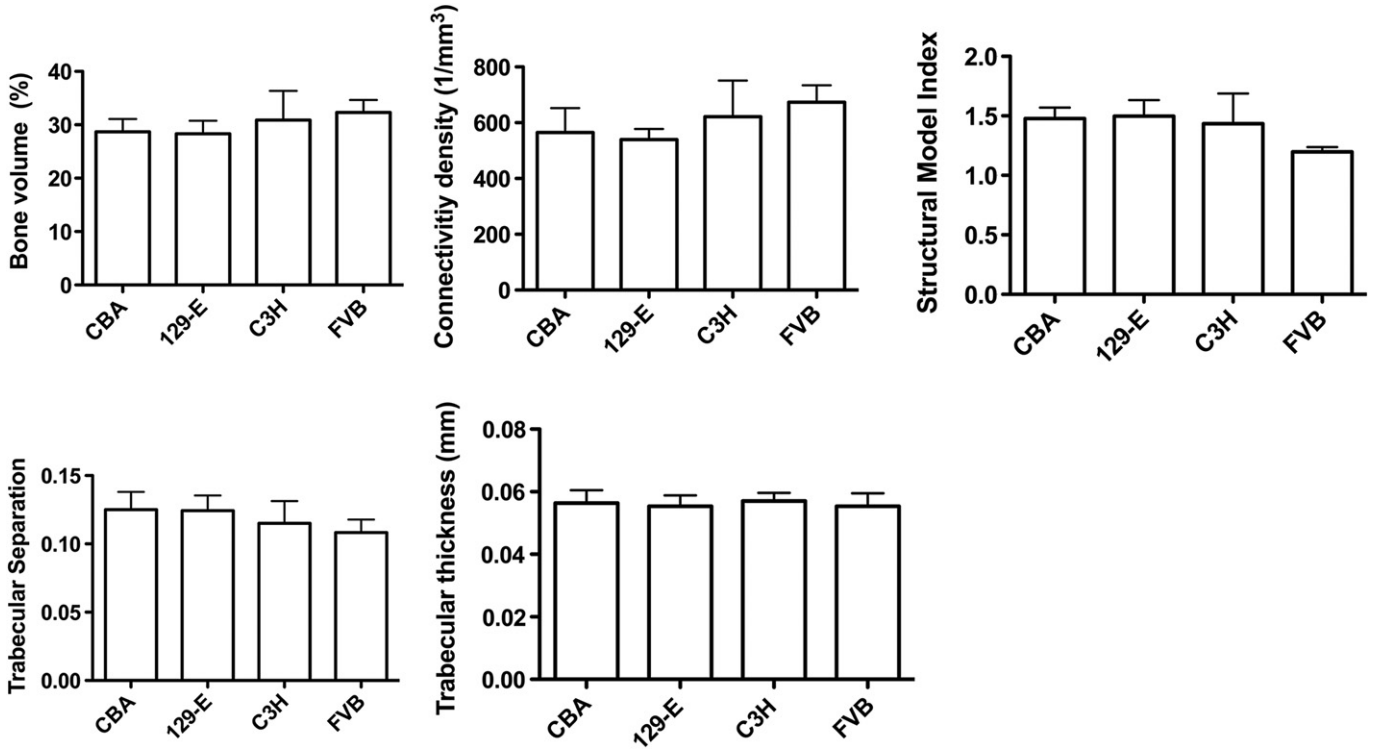

Fig. 5. Micro-CT scan femoral analysis. Femora of CBA, 129S2, C3H and FVB/NCrl were scanned with Micro-CT. After 3D digital reconstruction of the scanned images, a segment of the distal metaphysis was selected and several parameters calculated. There were no statistically significant differences for any of the parameters shown between the mouse strains. Statistical analysis was performed with One-Way ANOVA and Tukey's multiple comparison test ($p < 0.05$ and $n = 3$).

implantation, it is expected that the tissue at the periphery of the implant will be more vascularized than the tissue in the centre, since blood vessels do not immediately perfuse the whole implant. This led us to hypothesize that vascularization might be crucial (either triggering or sustaining) the biological mechanism that leads to osteoinduction by CaP ceramics in FVB mice. To address this hypothesis, we first investigated blood vessel formation occurring in TCP and BCP1150. Seven days after implantation,

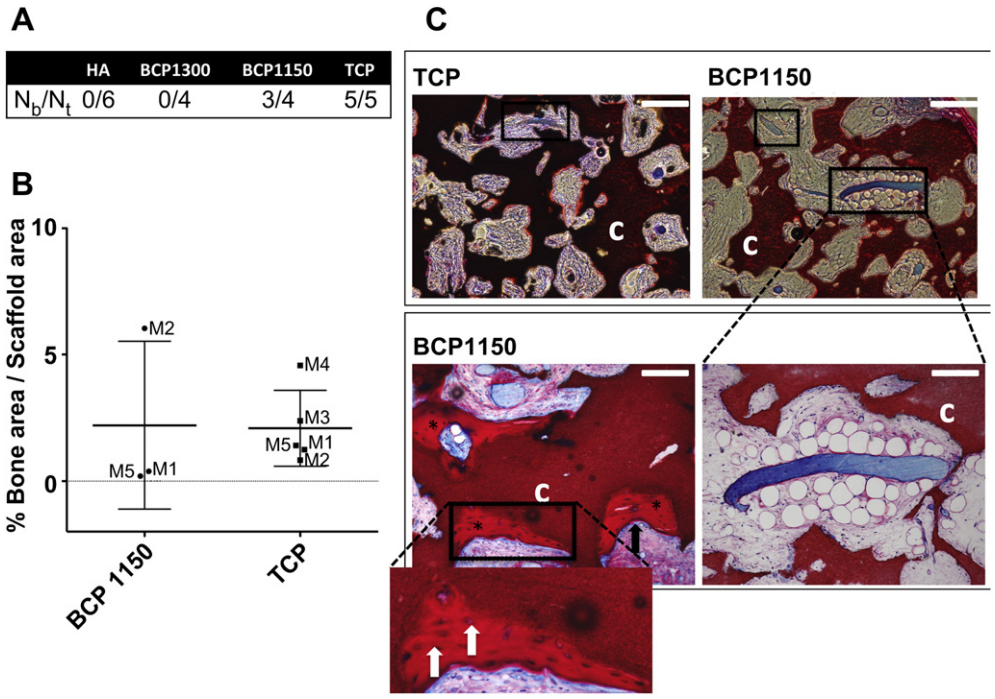

Fig. 6. Analysis of TCP, BCP1150, BCP1300 and HA explants after subcutaneous implantation in FVB mice for 12 weeks. A. Bone incidence in the different CaP ceramics shows that bone was only found in BCP1150 and TCP. B. There were no statistical differences regarding % bA/sA between TCP and BCP1150, as calculated with One-Way ANOVA with Tukey's multiple comparison test ($p < 0.05$). C. Representative images of tissue sections from TCP and BCP1150 explants. *Top panel* (scale bar represents 500 μm): notice presence of blood vessels (squares). *Bottom left*: mineralized bone tissue (asterisks) with osteoblasts (black arrow) and osteocytes (enlarged section); *Bottom right*: blood vessels surrounded by fat, characteristic of BCP1150 tissue sections. C: ceramic block. Scale bars represent 200 μm (A and B) and 100 μm (C).

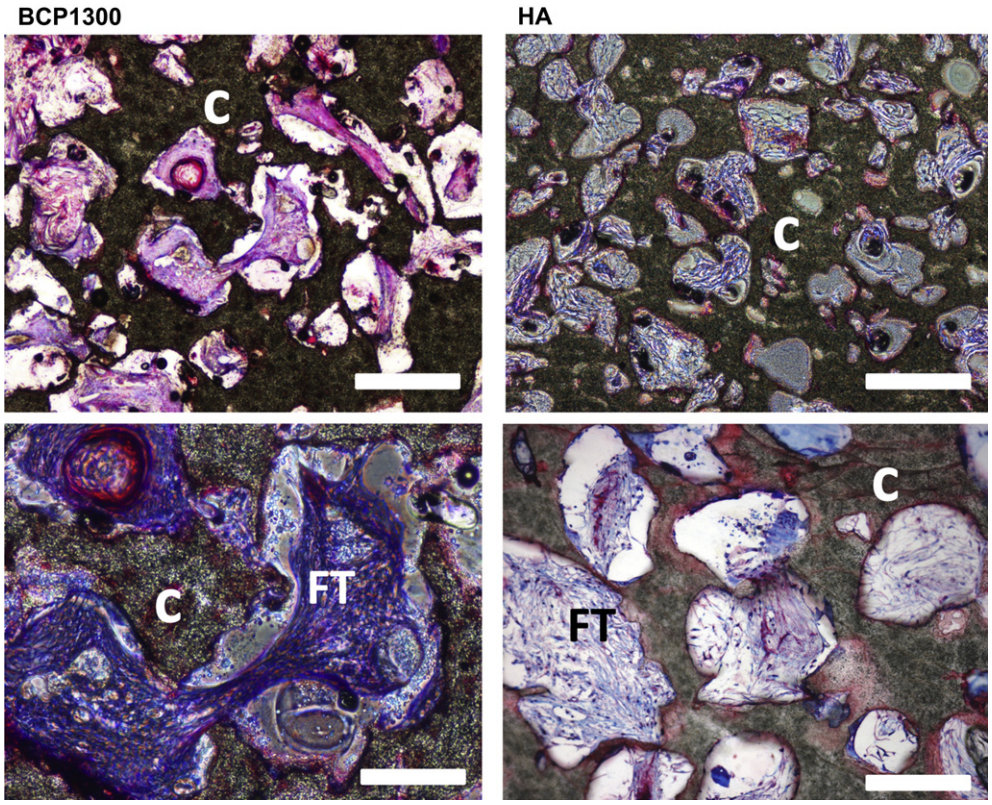

Fig. 7. Detailed images of BCP1300 and HA tissue explants 12 weeks after subcutaneous implantation in mice. Tissue locates preferentially in the center of the pores, loosely connected with the surface of both ceramic types. C: ceramic block FT = fibrous tissue. Scale bars represent 400 μm (top row) and 200 μm (bottom row).

mature blood vessels were observed in explants of both ceramics, evidenced by the presence of erythrocytes in the lumen (Fig. 8). After confirming that vascularization occurs rather quickly in these ceramics, next we analysed whether enhancing this early vascularization through addition of vascular endothelial growth factor (VEGF) to TCP, would increase the amount of bone formed. For this, all mice received one block of TCP (−VEGF) and one block of TCP with adsorbed VEGF (+VEGF) and these were explanted 12 weeks later. Our results showed that all explants with VEGF induced bone formation whereas only 4/5 without VEGF did (Fig. 8B). There were no statistically significant differences in the amount of bone formed between the two groups (Fig. 8C). Whereas TCP explants were well vascularized after 7 days of implantation, addition of VEGF to TCP prior to implantation did not increase amounts of bone formation as analysed 12 weeks later.

5. Discussion

In the search for a mouse model to study osteoinductive CaP ceramics, we tested 6–7 weeks old mice from 11 different inbred mouse strains (Table 1) for their responsiveness to subcutaneous implantation of TCP, based on the hypothesis that biomaterial-induced bone formation requires a particular genetic background.

Subcutaneous induction of bone formation by TCP was identified in two mouse strains: FVB and 129S2 (Fig. 4). Particularly in FVB, bone incidence (>80%) and amounts (2–3%) observed were never reported before [18], suggesting that this mouse strain is promising for the study of CaP osteoinductive ceramics.

Furthermore, TCP loaded with rhBMP-2 induced subcutaneous bone formation in all mouse strains but with amounts varying among them (Fig. 2). Taken together these data demonstrate that the genetic background influences the response to osteoinductive stimuli. Also considering that these are inbred mice, which are or are not susceptible to material-induced osteoinduction, potentiates the identification of genetic loci correlated with the mechanism.

Interestingly, FVB was the mouse strain in which bone formation induced by rhBMP-2 was lowest but when induced by TCP, highest, suggesting that the physiological mechanism causing the strain to strain variance is different between TCP and rhBMP-2. Furthermore, although in both cases bone tissue contained osteocytes and osteoblasts (Figs. 1 and 3), bone with bone marrow was observed in virtually all pores of the TCPb explants whereas it was only visible in some TCP pores, which is likely related to the amount of bone tissue formed.

Bone fracture healing capacity was also correlated with mouse genetic background [30,31]. Moreover, the bone regenerative capacity of different inbred mouse strains was strongly correlated with their BMD [31], although it was inversely correlated in another report [30]. Based on this, we analysed whether femoral BMD from different mouse strains was correlated to ectopic bone formation. However, femoral bone volume (Fig. 5) did not significantly differ among the strains tested, which could be due to the animals' age. We analysed femora from 1.5 months old mice and differences in BMD among different inbred strains have been reported at 2 months and thereafter [32].

Implantation of a series of CaP ceramics in FVB mice revealed that in order to observe bone formation after 12 weeks, a particular set of physico-chemical properties is required. HA, differing in terms of chemical composition and structural properties from TCP [3], did not induce bone formation. However, similar differences were observed between CaP ceramics with the same chemical composition but differing in terms of micro structural properties: whereas the more microporous BCP1150 induced bone formation, BCP1300 did not and moreover, the type of tissue found within the

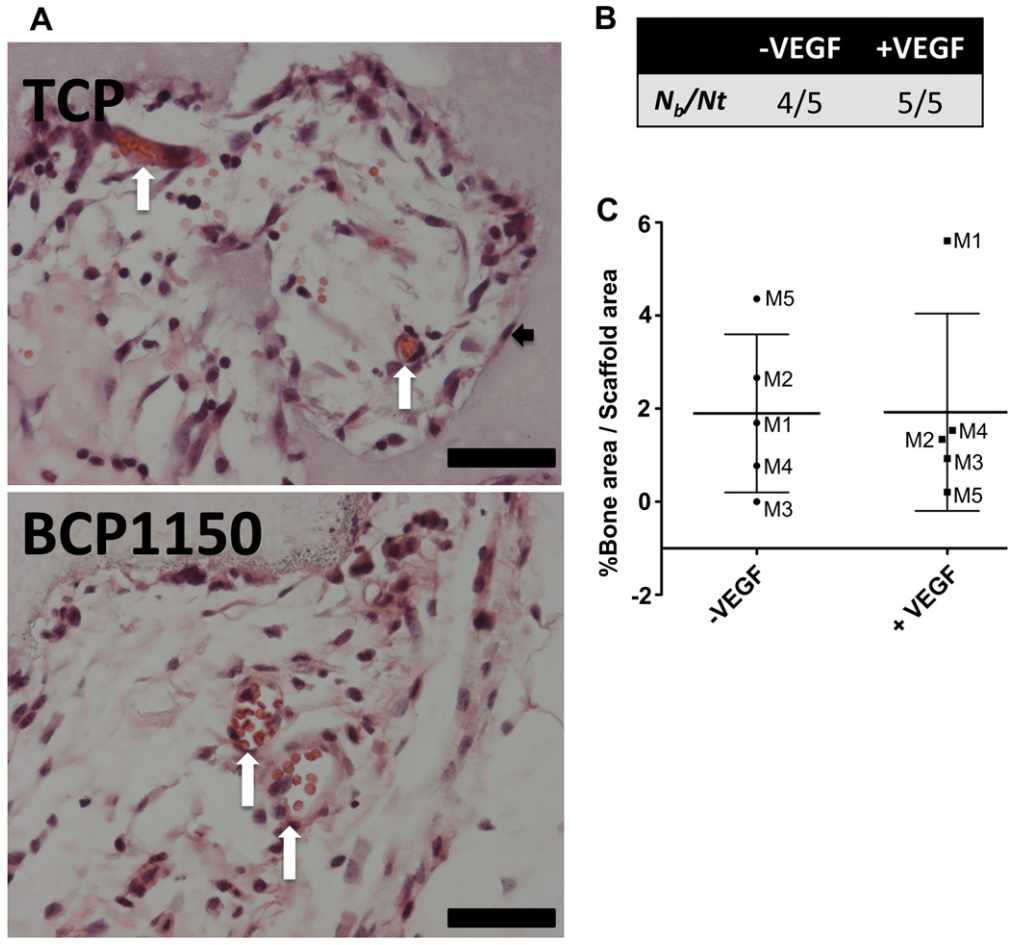

Fig. 8. Analysis of blood vessel formation and enhancement of vascularization in bone formation. A. Blood vessel formation in TCP and BCP1150 after 7 days subcutaneous implantation in FVB (white arrows). Notice cell alignment with TCP (black arrow). Scale bar represents 50 μm. Twelve weeks after subcutaneous implantation in FVB, N_b/N_t was higher in TCP (−VEGF) than in TCP with VEGF (+VEGF) (B) and there were no differences in % bA/sA (C). Statistical analysis was performed with One-Way ANOVA and Tukey's multiple comparison test ($p < 0.05$).

respective pores was very different (Figs. 6 and 7). These results suggest that microstructural properties determine attachment and spreading of cells in the pores and onto the surface, which might be determinant to whether bone will be deposited or not. Also, the osteoinductive potential revealed by the different CaP ceramics in FVB mice is similar to that seen in dogs, sheep and goats [2,3] from previous studies. Therefore we conclude that this mouse strain can be used as a model to investigate novel bone-inducing CaP ceramics.

Histological observations suggested that TCP and BCP1150 were more vascularized than BCP1300 and HA explants. Besides their demonstrated pro-osteogenic effects, it could be that TCP and BCP1150 also exert pro-angiogenic ones. In fact, it was shown that TCP and BCP induce higher vessel density than HA, up to 30 days after subcutaneous implantation in rats [33]. Furthermore, the effect of Ca^{2+} on angiogenesis has been reported [34–37], which could further indicate some relationship between Ca^{2+} dissolution from the CaP ceramics and blood vessel perfusion. Although this would not sustain the differences observed between BCP1150 and BCP1300, which possess similar dissolution rates [3], quantitative data is needed in order to support these statements.

Angiogenesis is also crucial for the process of bone formation [38] and some authors have suggested that the cells that are stimulated to deposit bone tissue in osteoinductive CaP ceramics are pericytes [13–15]. Our results show that blood vessels perfused both TCP and BCP1150 as early as 7 days, however enhancing angiogenesis at an early stage of implantation did not increase the abundance of bone tissue 12 weeks later (Fig. 8). As to the nature of the cells contributing to bone formation, we observed cells aligning with the material as early as 7 days (Fig. 8 and Fig. S3), which may be the osteoprogenitor cells, but whether these are derived from the walls of neighbouring blood vessels needs to be investigated.

The effect of surface characteristics on the inflammatory response by biomaterials has been reported. More specifically, the behaviour of macrophages can be tuned according to size, roughness or chemical composition of the biomaterials surface. For instance, Fellah and colleagues [11] showed that macrophage derived secretion of interleukin 6 and tumour necrosis factor α was dependent on BCP microparticle diameter in which they were cultured and that those cytokines could further induce osteogenic differentiation of MC3T3-E1 cells, suggesting a possible relation between inflammation and bone formation. Moreover, macrophages are susceptible to express BMP-2 in response to Ca^{2+} [39], which could also be correlated with the dissolution characteristics of these materials and their bone forming capacity. Although we did not address the functional role of macrophages in this study, we observed the presence of macrophages as early as 7 days in TCP (Fig. S3) and BCP1150. Some macrophages were also found in the vicinity of TCP and BCP1150 surfaces 12 weeks after implantation but higher amounts of these cells including numerous amounts of giant cells were found in the vicinity of HA and BCP1300 at that point in time (Fig. S3), suggesting that the innate inflammatory

response towards HA and BCP1300 is more pronounced than the one towards TCP and BCP1150. Regarding the adaptive immune response, also lymphocytes appearance on the surface of CaP implants has been linked with specific physico-chemical properties of materials [40]. However, in this study, CD20-positive B-cells were only sporadically found in the pores of BCP1150 and TCP (Fig. S3). Unfortunately, due to cross reaction with the murine tissue, CD3-positive cells could not be identified.

Besides having a promising role in the field of osteoinductive biomaterials, the FVB model could also boost research on the acquired form of heterotopic ossification (HO). HO is a debilitating disorder, usually induced by trauma or surgery, where pathological bone growth occurs in e.g. muscle tissue, or close to joints, resulting in deformation and impediment of normal movements [41–43]. Current drugs cannot effectively eliminate these excessive bone masses and typically affect normal bone as well [44]. Furthermore, current animal models do not provide a basis for solid research. Since the biological mechanism leading to HO is not fully understood, researchers do not know which relevant parameters should be included in an *in vivo* setup. Key physiological parameters believed to have a role in HO development are the nervous and immune systems, blood Ca^{2+} levels, O_2 levels in the tissue and disequilibrium of hormone levels, such as parathyroid hormone or calcitonin [45]. TCP implanted under the skin requires surgery and dissolves into the surrounding tissue, releasing Ca^{2+} ions, which are factors associated with HO onset. We think that the subcutaneous bone induction by TCP in FVB may also serve as a model for the acquired form of HO and could therefore be used to, for instance, investigate drugs to counteract ectopic bone formation.

6. Conclusions

In this study, we identified FVB as a mouse strain that is suitable for the investigation of osteoinductive CaP ceramics. Our experiments further demonstrate that the capacity of calcium phosphate ceramics to induce bone formation is dependent on the mouse genetic background, confirming that genetic and molecular mechanisms are determinant for osteoinduction to occur. Seemingly, bone induction by rhBMP-2 loaded onto TCP yielded amounts of bone formation dependent on inbred strain. Amounts of bone formation observed in both cases did not correlate with bone structural features, such as % bone volume, for any of the inbred strains tested. Bone induction by CaP ceramics in FVB is dependent on a specific set of physico-chemical properties. Ceramics with the same chemical composition but different microstructural properties yielded different results: BCP1150 induced bone formation whereas BCP1300 did not. HA also did not induce bone formation. Furthermore, although invaded by blood vessels at as early as day 7 after implantation, enhancing vascularization with VEGF did not increase amounts of bone formation by TCP.

Acknowledgements

The authors gratefully acknowledge the financial support of the TeRM Smart Mix Program of the Netherlands Ministry of Economic Affairs and the Netherlands Ministry of Education, Culture and Science. We also wish to acknowledge Annette Gijsbers-Bruggink and collaborators (Biobank, UMC Utrecht) and Liliana Teixeira, Joyce Doorn and Karolina Janeczek-Portalska for technical assistance.

Appendix A. Supplementary material

Supplementary data related to this article can be found online at doi:10.1016/j.biomaterials.2012.04.021.

References

[1] Huipin Y, Zongjian Y, Yubao L, Xingdong Z, Bruijn JDD, Groot KD. Osteoinduction by calcium phosphate biomaterials. J Mater Sci Mater Med 1998;9(12):723–6.
[2] Habibovic P, Yuan H, van der Valk CM, Meijer G, van Blitterswijk CA, de Groot K. 3D microenvironment as essential element for osteoinduction by biomaterials. Biomaterials 2005;26(17):3565–75.
[3] Yuan H, Fernandes H, Habibovic P, de Boer J, Barradas AM, de Ruiter A, et al. Osteoinductive ceramics as a synthetic alternative to autologous bone grafting. Proc Natl Acad Sci U S A 2010;107(31):13614–9.
[4] Ripamonti U, Crooks J, Kirkbride AN. Sintered porous hydroxyapatite with intrinsic osteoinductive activity: geometric induction of bone formation. S Afr J Sci 1999;95(8):335–43.
[5] Yamasaki H, Sakai H. Osteogenic response to porous hydroxyapatite ceramics under the skin of dogs. Biomaterials 1992;13(5):308–12.
[6] Carragee EJ, Hurwitz EL, Weiner BK. A critical review of recombinant human bone morphogenetic protein-2 trials in spinal surgery: emerging safety concerns and lessons learned. Spine J 2011;11(6):471–91.
[7] De Bruijn JD, Shankar K, Yuan HPH. Osteoinduction and its evaluation. In: Kokubo T, editor. Bioceramics and their applications. Cambridge: Woodhead Publishing Ltd; 2008. p. 199–219.
[8] Yoshida K, Oida H, Kobayashi T, Maruyama T, Tanaka M, Katayama T, et al. Stimulation of bone formation and prevention of bone loss by prostaglandin E EP4 receptor activation. Proc Natl Acad Sci U S A 2002;99(7):4580–5.
[9] Sakuma Y, Tanaka K, Suda M, Yasoda A, Natsui K, Tanaka I, et al. Crucial involvement of the EP4 subtype of prostaglandin E receptor in osteoclast formation by proinflammatory cytokines and lipopolysaccharide. J Bone Miner Res 2000;15(2):218–27.
[10] Harada Y, Wang JT, Doppalapudi VA, Willis AA, Jasty M, Harris WH, et al. Differential effects of different forms of hydroxyapatite and hydroxyapatite tricalcium phosphate particulates on human monocyte macrophages *in vitro*. J Biomed Mater Res 1996;31(1):19–26.
[11] Fellah BH, Delorme B, Sohier J, Magne D, Hardouin P, Layrolle P. Macrophage and osteoblast responses to biphasic calcium phosphate microparticles. J Biomed Mater Res A 2010;93A(4):1588–95.
[12] Thomsen P, Gretzer C. Macrophage interactions with modified material surfaces. Curr Opin Solid St M.5(2–3):163-176.
[13] Ripamonti U, Klar RM, Renton LF, Ferretti C. Synergistic induction of bone formation by hOP-1, hTGF-[beta]3 and inhibition by zoledronate in macroporous coral-derived hydroxyapatites. Biomaterials 2010;31(25):6400–10.
[14] Ripamonti U, Vandenheever B, Vanwyk J. Expression of the osteogenic phenotype in porous hydroxyapatite implanted extraskeletally in baboons. Matrix 1993;13(6):491–502.
[15] Yang Z, Yuan H, Tong W, Zou P, Chen W, Zhang X. Osteogenesis in extraskeletally implanted porous calcium phosphate ceramics: variability among different kinds of animals. Biomaterials 1996;17(22):2131–7.
[16] Hartman EHM, Vehof JWM, JEd Ruijter, Spauwen PHM, Jansen JA. Ectopic bone formation in rats: the importance of vascularity of the acceptor site. Biomaterials 2004;25(27):5831–7.
[17] Barradas AMC, Yuan H, van Blitterswijk CA, Habibovic P. Osteoinductive biomaterials: current knowledge of properties, experimental models and biological mechanisms. Eur Cell Mater 2011;21:407–29.
[18] Yuan H, van Blitterswijk CA, de Groot K, de Bruijn JD. Cross-species comparison of ectopic bone formation in biphasic calcium phosphate (BCP) and hydroxyapatite (HA) scaffolds. Tissue Eng 2006;12(6):1607–15.
[19] Yang RN, Ye F, Cheng LJ, Wang JJ, Lu XF, Shi YJ, et al. Osteoinduction by Ca-P biomaterials implanted into the muscles of mice. J Zhejiang Univ SCI B 2011; 12(7):582–90.
[20] Marusic A, Katavic V, Grcevic D, Lukic IK. Genetic variability of new bone induction in mice. Bone 1999;25(1):25–32.
[21] Li S, de Wijn JR, Li J, Layrolle P, de Groot K. Macroporous biphasic calcium phosphate scaffold with high permeability/porosity ratio. Tissue Eng 2003; 9(3):535–48.
[22] Yuan H, van den Doel M, Li S, van Blitterswijk CA, de Groot K, de Bruijn JD. A comparison of the osteoinductive potential of two calcium phosphate ceramics implanted intramuscularly in goats. J Mater Sci Mater Med 2002; 13(12):1271–5.
[23] Crouzier T, Sailhan Fdr, Becquart P, Guillot R, Logeart-Avramoglou D, Picart C. The performance of BMP-2 loaded TCP/HAP porous ceramics with a polyelectrolyte multilayer film coating. Biomaterials 2011;32(30):7543–54.
[24] Koyama N, Okubo Y, Nakao K, Osawa K, Bessho K. Experimental study of osteoinduction using a new material as a carrier for bone morphogenetic protein-2. Br J Oral Maxillofac Surg 2011;49(4):314–8.
[25] Hulsart-Billstrom G, Hu Q, Bergman K, Jonsson KB, Aberg J, Tang R, et al. Calcium phosphates compounds in conjunction with hydrogel as carrier for BMP-2: a study on ectopic bone formation in rats. Acta Biomater 2011;7(8):3042–9.
[26] Takahashi Y, Yamamoto M, Tabata Y. Enhanced osteoinduction by controlled release of bone morphogenetic protein-2 from biodegradable sponge composed of gelatin and beta-tricalcium phosphate. Biomaterials 2005; 26(23):4856–65.
[27] Matsushita N, Terai H, Okada T, Nozaki K, Inoue H, Miyamoto S, et al. A new bone-inducing biodegradable porous beta-tricalcium phosphate. J Biomed Mater Res A 2004;70A(3):450–8.

[28] Li JZ, Li H, Sasaki T, Holman D, Beres B, Dumont RJ, et al. Osteogenic potential of five different recombinant human bone morphogenetic protein adenoviral vectors in the rat. Gene Ther 2003;10(20):1735–43.
[29] Odgaard A. Three-dimensional methods for quantification of cancellous bone architecture. Bone 1997;20(4):315–28.
[30] Manigrasso M, O'Connor J. Comparison of fracture healing among different inbred mouse strains. Calcif Tissue Int 2008;82(6):465–74.
[31] Li X, Gu W, Masinde G, Hamilton-Ulland M, Rundle CH, Mohan S, et al. Genetic variation in bone-regenerative capacity among inbred strains of mice. Bone 2001;29(2):134–40.
[32] Beamer WG, Donahue LR, Rosen CJ, Baylink DJ. Genetic variability in adult bone density among inbred strains of mice. Bone 1996;18(5):397–403.
[33] Ghanaati S, Barbeck M, Detsch R, Deisinger U, Hilbig U, Rausch V, et al. The chemical composition of synthetic bone substitutes influences tissue reactions in vivo: histological and histomorphometrical analysis of the cellular inflammatory response to hydroxyapatite, beta-tricalcium phosphate and biphasic calcium phosphate ceramics. Biomed Mater 2012;7(1):015005.
[34] Andrikopoulos P, Baba A, Matsuda T, Djamgoz MBA, Yaqoob MM, Eccles SA. Ca2+ influx through reverse mode Na+/Ca2+ exchange is critical for vascular endothelial growth factor-mediated extracellular signal-regulated kinase (ERK) 1/2 activation and angiogenic functions of human endothelial cells. J Biol Chem 2011;286(44):37919–31.
[35] Jung HJ, Kim JH, Shim JS, Kwon HJ. A Novel Ca2+/calmodulin antagonist HBC inhibits angiogenesis and down-regulates hypoxia-inducible factor. J Biol Chem 2010;285(33):25867–74.
[36] Shen W-G, Peng W-X, Dai G, Xu J-F, Zhang Y, Li C- J. Calmodulin is essential for angiogenesis in response to hypoxic stress in endothelial cells. Cell Biol Int 2007;31(2):126–34.
[37] Mukhopadhyay D, Akbarali HI. Depletion of [Ca2+]i inhibits hypoxia-induced vascular permeability factor (vascular endothelial growth factor) gene expression. Biochem Biophys Res Commun 1996;229(3):733–8.
[38] Zelzer E, Olsen BR. Multiple roles of vascular endothelial growth factor (VEGF) in skeletal development, growth, and repair. Curr Top Dev Biol 2005;65:169–87.
[39] Honda Y, Anada T, Kamakura S, Nakamura M, Sugawara S, Suzuki O. Elevated extracellular calcium stimulates secretion of bone morphogenetic protein 2 by a macrophage cell line. Biochem Biophys Res Commun 2006;345(3):1155–60.
[40] Klein C, Patka P, Denhollander W. Macroporous calcium-phosphate bioceramics in dog femora - a histological study of interface and biodegradation. Biomaterials 1989;10(1):59–62.
[41] Shehab D, Elgazzar AH, Collier BD. Heterotopic ossification. J Nucl Med 2002;43(3):346–53.
[42] Potter BK, Forsberg JA, Davis TA, Evans KN, Hawksworth JS, Tadaki D, et al. Heterotopic ossification following combat-related trauma. J Bone Jt Surg Am 2010;92(Suppl. 2):74–89.
[43] Kan LX, Kessler JA. Animal models of typical heterotopic ossification. J Biomed Biotechnol 2011;2011:309289.
[44] Cullen N, Perera J. Heterotopic ossification: pharmacologic options. J Head Trauma Rehabil 2009;24(1):69–71.
[45] Baird EO, Kang QK. Prophylaxis of heterotopic ossification – an updated review. J Orthop Surg Res 2009;4:12.